Quantifying Human-Induced Dynamic and Thermodynamic Contributions to Severe Cold Outbreaks Like November 2019 in the Eastern United States

Chunlüe Zhou, Aiguo Dai, Junhong Wang, and Deliang Chen

AFFILIATIONS: Zhou and Dai—Department of Atmospheric and Environmental Sciences, University at Albany, State University of New York, Albany, New York; **Wang**—Department of Atmospheric and Environmental Sciences, and New York State Mesonet, University at Albany, State University of New York, Albany, New York; **Chen**—Regional Climate Group, Department of Earth Sciences, University of Gothenburg, Gothenburg, Sweden

CORRESPONDING AUTHOR: Dr. Chunlüe Zhou, chunluezhou@gmail.com

DOI:10.1175/BAMS-D-20-0171.1

A supplement to this article is available online (10.1175/BAMS-D-20-0171.2)

The eastern U.S. 2019 November cold outbreak was mainly caused by extreme northerly winds. CMIP6 results find nonsignificant dynamical effects of anthropogenic climate change on such regional winds; thermodynamic effects alone decreased the probability of this cold event by 70%.

In November 2019, although most of the world was anomalously warm (as the second warmest globally in November since 1900), 42 stations in the northeastern United States broke the historical record-low temperature since 1900 (stars in Fig. 1a). November average daily minimum temperatures (Tmin) at 536 stations in the eastern United States were below their 10th percentiles, in contrast to above-normal Tmin in the western United States (filled circles in Fig. 1a). This severe cold outbreak had a significant impact on society; for example, it increased residential energy consumption in the eastern United States by 84% in November 2019 relative to the 2000–18 November mean (https://www.ncdc.noaa.gov/societal-impacts/redti/).

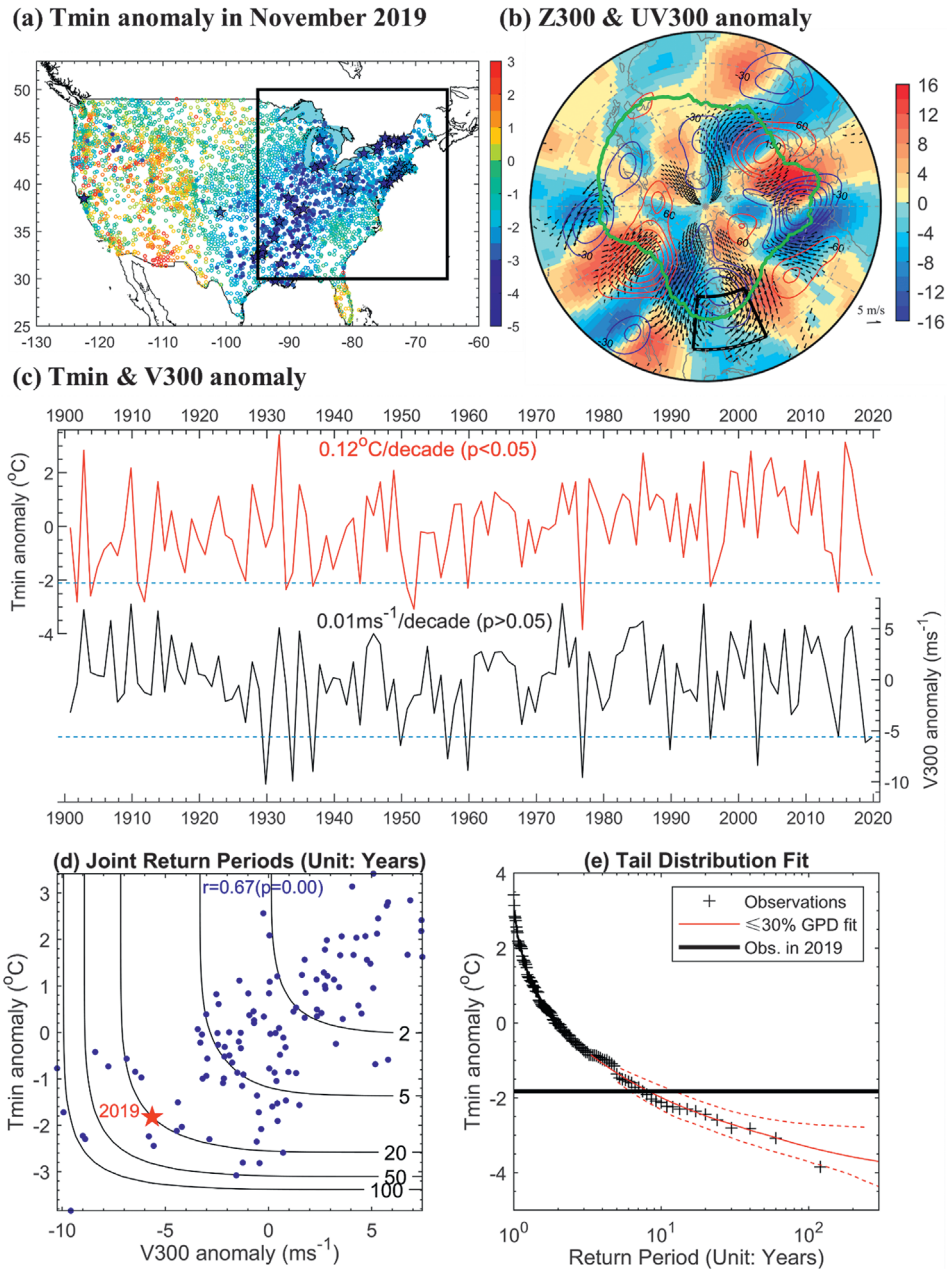

Fig. 1. (a) Spatial pattern of the average daily minimum air temperature (Tmin) anomalies (relative to 1900–2019 mean) in November 2019 over the contiguous United States. Stations marked respectively as stars and filled circles underwent the record-breaking and extremely low Tmin anomalies in November 2019 since 1900. Study region is shown as the black rectangle (for land areas only). (b) The 300-hPa geopotential height anomalies (Z300; red/blue contours with a 30-m interval) and meridional wind anomalies (V300; color shading; m s^{-1}) in November 2019. The 300-hPa wind anomalies regressed onto the November 2019 Tmin anomalies are shown as arrows for areas where regressions of the V300 anomalies are significant at the 5% level. The average jet stream position with maximum wind speed is shown as a green contour. The region for the average V300 anomalies is shown as the black frame. (c) Time series of regional average Tmin and V300 anomalies. Trends are shown at the middle. The 10th percentile line is shown as light blue horizontal line. (d) Joint return periods (contours) of the observed Tmin and V300 anomalies (blue dots). The 2019 values are shown as a red star. Note that the weak winds during the five cold events are related to the uncertainty of reanalysis V300 during the early period, i.e., 1900–30. (e) Generalized Pareto distribution (GPD) fit (red; dashed line for 5%–95% confidence intervals) of the observed November Tmin anomalies (black pluses).

For the past regional cold air outbreaks, a persistent and meandering anomalous polar jet stream was found to propagate the Arctic cold air into many parts of the eastern United States through anomalous northerlies (Francis et al. 2017; Cohen et al. 2018; Xie et al. 2019). Global warming raises the background mean temperature, which increases the frequency of the warm events but decreases the chance of cold events, especially in regions north of 50°N where surface warming has been the largest (Alexander et al. 2006; Hartmann et al. 2013; Christiansen et al. 2018). However, the frequency of winter extreme cold events in the eastern United States and some Eurasian regions has increased in recent decades, especially in mid- to late winter (Scherer and Diffenbaugh 2014; Cohen et al. 2018). These increases in cold extremes have been mainly attributed to changes in the frequency of certain weather patterns that displace cold airmasses southward to different sectors of the northern midlatitudes (Zhou ang Wang 2016; Singh et al. 2016; Deng et al. 2020; Luo et al. 2020). However, whether recent global warming has contributed to the weather pattern change remains unknown.

While the thermodynamic effect of global warming alone is expected to increase warm event frequencies, it cannot directly explain the increased cold events. Based on our prior work of regional heat wave attribution (Zhou et al. 2020), in addition to estimating the role of anomalous northerlies, we also attempted to quantify the roles of human influences in the probability of the eastern U.S. 2019 cold outbreak from both dynamic and thermodynamic perspectives. Our results should provide a physical way to reconcile the interpretations of human influences on warm and cold events.

In summary, this study tries to answer three questions: 1) What does the eastern U.S. 2019 November cold air outbreak look like in the historical context? 2) How much do the anomalous northerlies contribute to the probability of severe cold outbreaks like this one? 3) What are relative roles of human-induced dynamic and thermodynamic changes in shaping severe cold events like November 2019 over the eastern United States?

Data and methods.

To show the 2019 cold event in historical context and its spatial pattern, we used the November Tmin monthly data at ~1,600 stations with more than 30 years of data from 1900 to 2019 in the study region (land areas within 65°–95°W, 30°–50°N; Fig. 1a) from the latest Berkeley homogenized observation dataset (available at http://berkeleyearth.org/) (Muller et al. 2013). This temperature dataset was homogenized by comparing with nearest neighbor stations (Muller et al. 2013) and employed in studying regional extremes (Zhou and Wang 2016).

To depict the atmospheric circulation pattern behind the event, we used the 1° × 1° 300 hPa geopotential height (Z300), zonal wind (U300), and meridional wind (V300) data from NOAA-20CRv3 (the Twentieth Century Reanalysis version 3 produced by the National Oceanic and Atmospheric Administration) from 1900 to 2015 (available at https://www.esrl.noaa.gov/psd/data) (Slivinski et al. 2019). These data were extended to 2019 using JRA-55 (the 55-Year Japanese Re-Analysis) reanalysis data (available at http://jra.kishou.go.jp/) (Kobayashi et al. 2015) by correcting their 1958–2015 mean differences. Jet stream position is shown here as the November average latitude (northward of 30°N) where the 6-hourly wind speed at 300 hPa reaches its maximum (Fig. 1b).

Monthly outputs from the models participated in CMIP6 (phase 6 of the Coupled Model Intercomparison Project Phase 6; https://esgf-node.llnl.gov/search/cmip6/) (Eyring et al. 2016) were used to quantify human influences on the probability of the eastern U.S. 2019 cold air outbreak. Twenty out of 29 CMIP6 historical all-forcings (ALL; see Table ES1 in the supplemental material) runs were selected in this study because of (i) comparable histograms ($p > 0.05$ via a Kolmogorov–Smirnov test) of the November Tmin (V300) anomalies between CMIP6 ALL runs and observations (reanalyses), and (ii) significant ($p < 0.05$) positive temporal correlations between the detrended Tmin and V300 anomalies from CMIP6 ALL runs and observations. The Tmin and V300

anomaly series and their trends during 1900–2019 are shown in Fig. ES1. To better represent the current climate for the 2019 event and consider sample size, we used a centered 40-yr window (2000–39) to represent climate conditions circa 2019 consisting of the selected ALL runs and the extended Shared Socioeconomic Pathway 2_45 (SSP2_45) runs. The resampled data from natural-forcings-only (NAT) runs (Table ES1) were adopted for comparison.

To be consistent, all the data were converted into anomalies relative to the 1900–2019 mean. Observations were first averaged onto 1° × 1° grids and model data were interpolated into the 1° × 1° observation grids using bilinear interpolation; they were then averaged (with area as weight) over the study region. To estimate the occurrence probability of the event, we constructed the probability density function (PDF) of the November Tmin and V300 anomalies using a Gaussian kernel estimate for the interior and a generalized Pareto distribution (GPD) estimate for the upper and lower tails. The boundaries of the lower and upper tails are the 30th and 70th percentiles. A Student's *t* copula (Demarta and McNeil 2005) was used to derive a correlation between their fitted probability distributions.

To estimate the regional circulation changes induced by human influences, following Zhou et al. (2019), we calculated the probability ratio (PR) of the V300 anomalies at or below the 2019 regional mean value (≤–5.64 m s^{-1} from reanalysis) between the ALL and NAT runs. The November Tmin anomalies were decomposed into dynamic and thermodynamic parts. The dynamic part was calculated by regressing the regional mean November Tmin anomalies onto the V300 anomalies and the local thermodynamic part is the residual. We used the V300-related Tmin variations to represent the circulation-induced or dynamic contribution, even though a circulation change would advect airmasses with different thermodynamic properties such as air temperature and humidity. To further quantify the human-induced dynamic and thermodynamic contributions to the probability of the eastern U.S. 2019 cold outbreak, we respectively calculated the PRs of the dynamic and thermodynamic parts at or below the 2019 values when anomalous northerlies (≤–5.64 m s^{-1}) occur in ALL and NAT runs. The 95% confidence intervals (CI) were estimated with a 10,000-member bootstrap (with replacement).

Results.

The 2019 November cold air outbreak in historical context. In November 2019, 300-hPa meridional wind anomalies exhibited a meandering planetary-scale wave pattern over the northern mid- to high latitudes (color shading in Fig. 1b), with anomalous northerlies over North America (arrows at a significance level of 0.05 in Fig. 1b). The persistent wavier polar jet stream pushed cold air masses from Canada down across the Great Lakes, and then into the central and northeastern United States (green contour in Fig. 1b), leading to a cold air outbreak over the eastern United States (Fig. 1a).

The Tmin anomaly averaged over the eastern United States is –1.82°C in November 2019, close to the 10th percentile during 1900–2019 (Fig. 1c). The PDF fit of the observed November Tmin anomalies suggests that the eastern U.S. 2019 cold outbreak is a 1-in-8-yr event (95% CI: 1 in 6–12 yr) (Fig. 1e). The detrended November Tmin anomalies show a significant correlation ($r = 0.70$, $p < 0.001$) with the detrended V300 anomalies over the region 90°–120°W, 40°–60°N. A Student's *t* copula fit suggests the November Tmin and V300 anomalies have a 1-in-20-yr concurrent return period (Fig. 1d).

Role of anomalous northerlies. To identify the roles of anomalous northerlies in the eastern U.S. 2019 cold outbreak, we estimated the probabilities of the November Tmin anomalies at or below the 2019 value (≤–1.82°C) for two cases in CMIP6 ALL runs: one with strong northerly winds (i.e., V300 ≤ –5.64 m s^{-1}; red in Fig. 2c) and one with neutral or weak winds (i.e., –1 ≤ V300 ≤ 1 m s^{-1}; gray in Fig. 2c). They are 0.273 (95% CI: 0.12–0.36) and 0.014 (95% CI: 0.01–0.03) (Fig. 2c), respectively. Thus, the chance for such

a cold outbreak event to occur over the eastern United States under strong northerlies is approximately 18 times (PR; 95% CI: 7–55 times) that under weak winds (Fig. 2e). This suggests a crucial role of northerly wind in causing winter cold outbreak over the eastern United States, as the northerly wind advects cold air from Canada into the central and eastern United States (Fig. 1b). The large uncertainty in this PR is mainly ascribed to low event probability and its large uncertainty during weak winds (Fig. 2e).

Human-induced dynamic and thermodynamic contributions. Figures 2a and 2b show a significant lower probability in CMIP6 ALL runs than in NAT runs for the November Tmin anomalies to be ≤–1.82°C, but a nonsignificantly higher probability for the November V300 anomalies to be ≤–5.64 m s^{-1}. Their PRs are 0.23 (95% CI: 0.16–0.31) and 1.25 (95% CI: 0.91–1.95), respectively. This suggests that human influences might tend to increase the occurrence frequency of the anomalous northerlies and thus the likelihood of the cold outbreak events, which could partly offset United States.

We further focused on estimating human influences for the cases with V300 ≤ –5.64 m s^{-1}, which represent conditions with strong northerlies like that in November

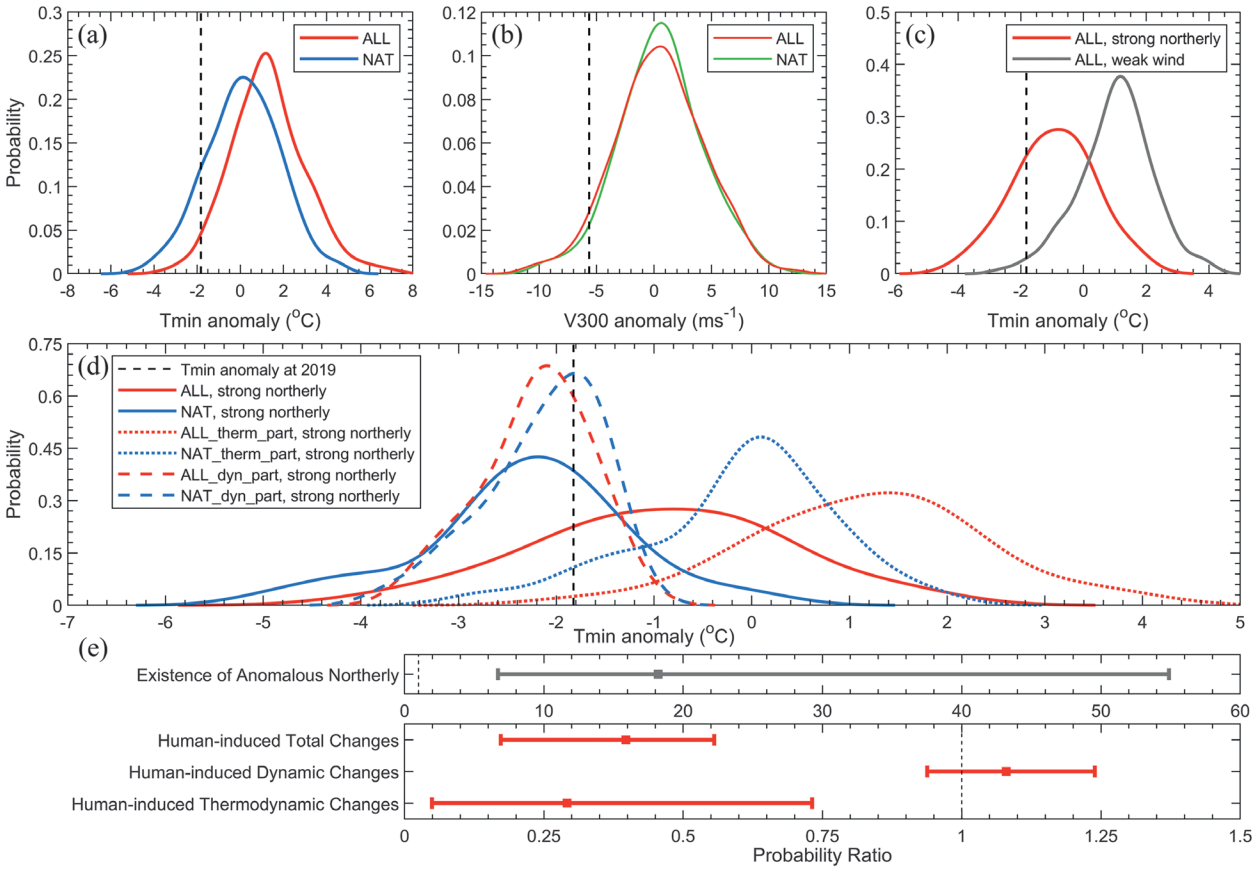

Fig. 2. (a) Estimated probability density functions (PDFs) of the November average daily minimum air temperature (Tmin) anomalies averaged over the eastern United States during a 40-yr window (2000–39) simulated by 20 CMIP6 models under the all-forcing (ALL; red) and natural-forcing-only (NAT; blue) scenarios. The observed value for November 2019 is shown as the black vertical line. The PDF plots were smoothed by kernel density function with 200 equallys spaced points. (b) As in (a), but for V300 anomalies (dashed line from reanalysis). (c) As in (a), but for two cases in the ALL runs: with strong northerly winds (V300 ≤ –5.64 m s^{-1}, the value in November 2019; red) and one with wind winds (–1 ≤ V300 ≤ 1 m s^{-1}; gray). (d) As in (a), but for cases with strong northerly winds in the ALL and NAT runs (solid curves; unit: %). These two PDFs are further decomposed into a dynamic (dashed curves) and a thermodynamic part (dot lines) (see text for details). (e) Probability ratios (PR) between the CMIP6 ALL and NAT runs of the cold outbreaks like November 2019 due to the occurrence of northerlies (gray) and human influences (red). The human influences are also estimated for the dynamic and thermodynamic parts.

2019. For these cases with strong northerlies, we compared the probabilities for the November Tmin anomalies to be ≤ –1.82°C in the ALL and NAT runs (solid red and blue curves, respectively, in Fig. 2d), and found that their PR is 0.40 (95% CI: 0.17–0.56; Fig. 2e). This indicates that human influences might have decreased the probability of the eastern U.S. 2019 cold air outbreak by ~60%.

To better understand human influences on the 2019 event in a physical way, we further quantified the contributions from the dynamic and thermodynamic perspectives. We first decomposed the November Tmin anomalies into the dynamic and thermodynamic parts (as described above). We then calculated the PRs between the ALL and NAT runs for the dynamic and thermodynamic parts of the Tmin anomalies at or below the 2019 values for cases with anomalous northerlies (i.e., V300 ≤ –5.64 $m \cdot s^{-1}$) (dashed and dotted lines in Fig. 2d) and found the PRs to be 1.08 (95% CI: 0.95–1.24) and 0.30 (95% CI: 0.05–0.73) for the dynamic and thermodynamic parts, respectively (Fig. 2e). In other words, the human-induced dynamic (i.e., northerly wind) changes increase the chance (by ~8%, nonsignificant at a level of 0.05) of severe cold outbreaks like November 2019 over the eastern United States, while the human-induced thermodynamic changes alone decrease their chance by ~70%. Note that the larger PR uncertainty for the thermodynamic part than for the dynamic part may be related to the use of the V300-regressed Tmin variations as the dynamic part and the residual as the thermodynamic part, since the V300-regressed Tmin variations only represent the effect from large-scale circulation (see section "Data and methods").

Summary.

The eastern United States experienced a cold air outbreak in November 2019 with regional-mean Tmin anomaly (–1.82°C) close to the 10th percentile of 1900–2019. Our analyses of observations and reanalysis show that extreme northerly winds (≤–5.64 $m\ s^{-1}$) were a principal factor responsible for this cold outbreak. An analysis of CMIP6 model data further suggests that the existence of such anomalous northerlies can increase the probability of such cold outbreaks to about 18 times compared with cases with weak winds (–1 ≤ V300 ≤ 1 $m\ s^{-1}$).

Comparing the probabilities of such cold outbreaks under conditions with strong anomalous northerlies (V300 ≤ –5.64 $m \cdot s^{-1}$) in CMIP6 ALL and NAT runs, we found that human influences might have decreased the likelihood of such cold outbreaks by ~60% (95% CI: 44%–83%). The analyses of the V300-based regressions and event probability ratios further indicate that the human-induced dynamic (i.e., northerly wind) changes might have increased the likelihood of such events by 8% (nonsignificant at a level of 0.05), whereas the human-induced thermodynamic changes might have decreased the chances of the events by 70%. This event attribution helps us to better understand the roles of human influences on the formation and evolution of the cold air outbreaks over the eastern United States.

Acknowledgments. This study was supported the U.S. National Oceanic and Atmospheric Administration (NA18OAR4310425). A. Dai was also supported by the National Science Foundation (OISE-1743738). Dr. Martin P. Hoerling and three anonymous reviewers are thanked for providing constructive reviews to improve the paper.

References

Alexander, L., and Coauthors, 2006: Global observed changes in daily climate extremes of temperature and precipitation. *J. Geophys. Res.*, **111**, D05109, https://doi.org/10.1029/2005JD006290.

Christiansen, B., and Coauthors, 2018: Was the cold European winter of 2009/10 modified by anthropogenic climate change? An attribution study. *J. Climate*, **31**, 3387–3410, https://doi.org/10.1175/JCLI-D-17-0589.1.

Cohen, J., K. Pfeiffer, and J. A. Francis, 2018: Warm Arctic episodes linked with increased frequency of extreme winter weather in the United States. *Nat. Commun.*, **9**, 869, https://doi.org/10.1038/s41467-018-02992-9.

Demarta, S., and A. J. McNeil, 2005: The t copula and related copulas. *Int. Stat. Rev.*, **73**, 111–129, https://doi.org/10.1111/j.1751-5823.2005.tb00254.x.

Deng, J., A. Dai, and D. Chyi, 2020: Northern Hemisphere winter air temperature patterns and their associated atmospheric and ocean conditions. *J. Climate*, **33**, 6165–6186, https://doi.org/10.1175/JCLI-D-19-0533.1.

Eyring, V., S. Bony, G. A. Meehl, C. A. Senior, B. Stevens, R. J. Stouffer, and K. E. Taylor, 2016: Overview of the Coupled Model Intercomparison Project phase 6 (CMIP6) experimental design and organization. *Geosci. Model Dev.*, **9**, 1937–1958, https://doi.org/10.5194/gmd-9-1937-2016.

Francis, J. A., S. J. Vavrus, and J. Cohen, 2017: Amplified Arctic warming and mid-latitude weather: New perspectives on emerging connections. *Wiley Interdiscip. Rev.: Climate Change*, **8**, e474, https://doi.org/10.1002/wcc.474.

Hartmann, D. L., and Coauthors, 2013: Observations: Atmosphere and surface. Climate Change 2013: The Physical Science Basis, Cambridge University Press, 159–254.

Kobayashi, S., and Coauthors, 2015: The JRA-55 reanalysis: General specifications and basic characteristics. *J. Meteor. Soc. Japan*, **93**, 5–48, https://doi.org/10.2151/jmsj.2015-001.

Luo, B., D. Luo, A. Dai, I. Simmonds, and L. Wu, 2020: Combined influences on North American winter air temperature variability from North Pacific blocking and the North Atlantic Oscillation. *J. Climate*, **33**, 7101–7123, https://doi.org/10.1175/JCLI-D-19-0327.1.

Muller, R. A., and Coauthors, 2013: Earth atmospheric land surface temperature and station quality in the contiguous United States. *Geoinfor. Geostat.*, **1**, 3, https://doi.org/10.4172/2327-4581.1000107.

Scherer, M., and N. S. Diffenbaugh, 2014: Transient twenty-first century changes in daily-scale temperature extremes in the United States. *Climate Dyn.*, **42**, 1383–1404, https://doi.org/10.1007/s00382-013-1829-2.

Singh, D., D. L. Swain, J. S. Mankin, D. E. Horton, L. N. Thomas, B. Rajaratnam, and N. S. Diffenbaugh, 2016: Recent amplification of the North American winter temperature dipole. *J. Geophys. Res. Atmos.*, **121**, 9911–9928, https://doi.org/10.1002/2016JD025116.

Slivinski, L. C., and Coauthors, 2019: Towards a more reliable historical reanalysis: Improvements for version 3 of the Twentieth Century Reanalysis system. *Quart. J. Roy. Meteor. Soc.*, **145**, 2876–2908, https://doi.org/10.1002/qj.3598.

Xie, Z., R. X. Black, and Y. Deng, 2019: Planetary and synoptic-scale dynamic control of extreme cold wave patterns over the United States. *Climate Dyn.*, **53**, 1477–1495, https://doi.org/10.1007/s00382-019-04683-7.

Zhou, C., and K. Wang, 2016: Coldest temperature extreme monotonically increased and hottest extreme oscillated over Northern Hemisphere land during last 114 years. *Sci. Rep.*, **6**, 25721, https://doi.org/10.1038/srep25721.

——, ——, D. Qi, and J. Tan, 2019: Attribution of a record-breaking heatwave event in summer 2017 over Yangtze River Delta. *Bull. Amer. Meteor. Soc.*, **100** (1), S97–S103, https://doi.org/10.1175/BAMS-D-18-0134.1.

——, D. Chen, K. Wang, A. Dai, and D. Qi, 2020: Conditional attribution of the 2018 summer extreme heat over Northeast China: Roles of urbanization, global warming, and warming-induced circulation changes. *Bull. Amer. Meteor. Soc.*, **101** (1), S71–S76, https://doi.org/10.1175/BAMS-D-19-0197.1.